

# Crystal structures and magnetic properties of two alternating azide-bridged complexes $[\{M(\text{dmbpy})(\text{N}_3)_2\}_n]$ ( $M = \text{Mn}$ or $\text{Cu}$ ; $\text{dmbpy} = 4,4'$ -dimethyl-2,2'-bipyridine) †

Zhen Shen,<sup>a</sup> Jing-Lin Zuo,<sup>\*a</sup> Zhi Yu,<sup>a</sup> Yong Zhang,<sup>a</sup> Jun-Feng Bai,<sup>a</sup> Chi-Ming Che,<sup>b</sup> Hoong-Kun Fun,<sup>c</sup> Jagadese J. Vittal<sup>d</sup> and Xiao-Zeng You<sup>\*a</sup>

<sup>a</sup> Coordination Chemistry Institute, State Key Laboratory of Coordination Chemistry, Nanjing University, Nanjing 210093, P. R. China

<sup>b</sup> Department of Chemistry, The University of Hong Kong, Pokfulam Road, Hong Kong

<sup>c</sup> X-Ray Crystallography Unit, School of Physics, Universiti Sains Malaysia, 11800 USM, Penang, Malaysia

<sup>d</sup> Department of Chemistry, National University of Singapore, Lower Kent Ridges Road, 119260, Singapore

Received 18th May 1999, Accepted 30th July 1999

Single crystals of complexes  $[\{\text{Mn}(\text{dmbpy})(\text{N}_3)_2\}_n]$  **1** and  $[\{\text{Cu}(\text{dmbpy})(\text{N}_3)_2\}_n]$  **2** ( $\text{dmbpy} = 4,4'$ -dimethyl-2,2'-bipyridine) were obtained from aqueous solutions containing 4,4'-dimethyl-2,2'-bipyridine, metal ions and sodium azide, and their structures determined by X-ray diffraction methods. The structure of **1** is a neutral two-dimensional network in which each  $\text{Mn}^{\text{II}}$  is bridged to three other metal ions through alternating single end-to-end and double end-on azido bridges. Compound **2** is a neutral chain in which the  $\text{Cu}^{\text{II}}$  is alternately bridged by double asymmetrical end-on and end-to-end azide groups. The magnetic properties of **1** and **2** have been investigated in the temperature range 5–300 K. Alternating ferro- and antiferro-magnetic interactions exist in the two compounds. A theoretical model has been developed for an  $S = 5/2$  alternating ferromagnetic–antiferromagnetic coupled 2-D system: the exchange parameters obtained with this model are  $J/k = -7.7$  K,  $zJ'/k = 2.5$  K and  $g = 2.0$  for **1**. An  $S = 1/2$  alternating ferromagnetic–antiferromagnetic coupled chain with the spin Hamiltonian  $H = -J_1 \sum S_{2i} \cdot S_{2i+1} - J_2 \sum S_{2i+1} \cdot S_{2i+2}$  leads to:  $J_1/k = 11$  K,  $J_2/k = -87$  K and  $g = 2.06$  for **2**. The natures and the magnitude of the alternating ferro- and antiferro-magnetic interactions in both compounds are discussed based on their structures.

## Introduction

In recent years chemists have paid much attention to molecular-based materials containing simultaneous ferro- and antiferromagnetic interactions. Several synthesis strategies in designing these complexes have been proposed recently.<sup>1–12</sup> Of these strategies, azide ion has been selected for the versatility of this ligand to allow ferro- or antiferro-magnetic coupling according to its co-ordination mode (end-on EO or end-to-end EE) to the transition metals. From the magnetic point of view, the end-to-end mode gives rise to antiferromagnetic interactions, while the end-on mode promotes ferromagnetic interactions between the metal ions even for  $\text{Mn}^{\text{II}}$  with  $S = 5/2$ .<sup>6</sup> The ferromagnetic behavior in the compounds with EO bridges has been explained by the spin-polarization concept<sup>13</sup> for angles between 100 and 105°. The different magnetic behavior caused by the two kinds of azide bridges, which is general for different metal ions, allows the possibility of obtaining compounds with alternating ferro- and antiferro-magnetic interactions. To date, systems containing both end-on and end-to-end azide groups have been reported with the aim of studying their magnetostructural correlation. These systems include the 1-D,<sup>1,8,9</sup> 2-D,<sup>2,3,4</sup> and 3-D<sup>2</sup> manganese(II) compounds with alternating EO and EE bridges, an alternating azide bridged copper(II) chain,<sup>14</sup> a 2-D nickel(II) complex<sup>6</sup> containing alternating EO and EE bridges and chains of  $\text{Ni}^{\text{II}}$ ,  $\text{Co}^{\text{II}}$ ,  $\text{Fe}^{\text{II}}$  or  $\text{Mn}^{\text{II}}$  with alternating EO and EE bridges.<sup>9</sup> Alternating ferro- and antiferromagnetic interaction is

still a rare phenomenon in molecular-based magnetic materials. To our knowledge, two- (2-D) or three-dimensional (3-D) systems showing this kind of magnetic interaction are few. To obtain materials with unusual magnetic properties derived from the azide group, we present here two new complexes with alternating end-on and end-to-end azide bridges and use developed theoretical models to correlate molecular structures with magnetic properties.

## Experimental

### Materials

Manganese(II) nitrate hexahydrate, copper(II) dichloride hexahydrate, 4,4'-dimethyl-2,2'-bipyridine and sodium azide were purchased from commercial sources and used as received.

### Physical techniques

Elemental analyses for C, H and N were performed on a Perkin-Elmer 240C analyzer. The IR spectra were taken on a Nicolet-170SX FT-IR spectrophotometer with KBr pellets in the range 4000–400  $\text{cm}^{-1}$ , EPR spectra using a Bruker 2000-SRC spectrometer. Variable-temperature magnetic susceptibility measurements were performed on polycrystalline samples in the temperature range 5–300 K in fields of 10 kOe with a SQUID Quantum Design MPMS-7 magnetometer. Susceptibilities were corrected for diamagnetism using Pascal constants as  $-184 \times 10^{-6}$   $\text{emu mol}^{-1}$  (**1**) and  $-133 \times 10^{-6}$   $\text{emu mol}^{-1}$  (**2**) and the temperature independent paramagnetism estimated at  $60 \times 10^{-6}$   $\text{emu mol}^{-1}$  per copper(II) ion for **2**. Our analyses did not include any zero-field splitting.

† Supplementary data available: rotatable 3-D crystal structure diagram in CHIME format. See <http://www.rsc.org/suppdata/dt/1999/3393/>

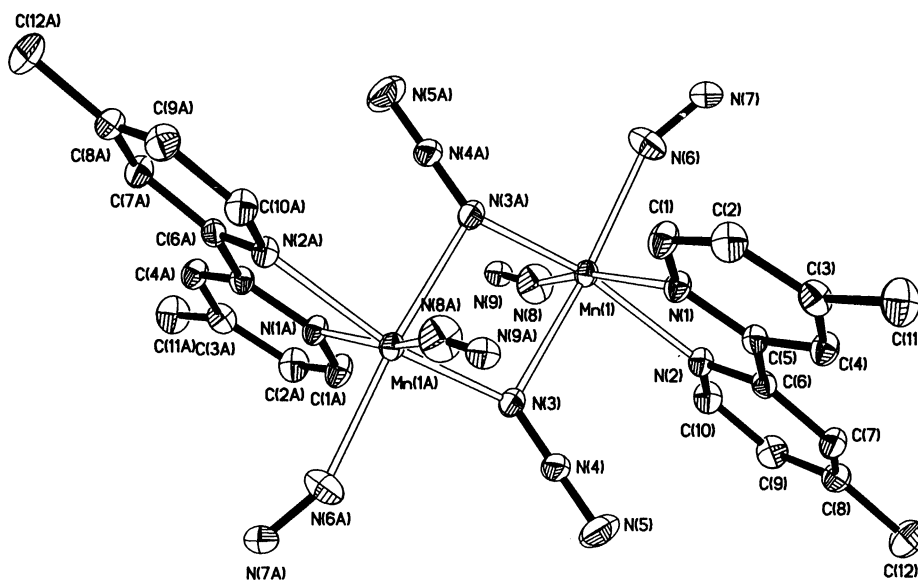


Fig. 1 An ORTEP drawing (30% thermal probability ellipsoids) of  $[\{\text{Mn}(\text{dmbpy})(\text{N}_3)_2\}_n] \mathbf{1}$  showing the atom numbering.

### Crystal structure determination

A summary of the crystal data collection and refinement parameters for compounds **1** and **2** is given in Table 1. Single crystals of approximate dimensions  $0.2 \times 0.2 \times 0.1$  (**1**) and  $0.38 \times 0.36 \times 0.3$  mm (**2**) were put on a Siemens SMART CCD diffractometer. Intensity data were collected at room temperature using graphite monochromated Mo-K $\alpha$  radiation ( $\lambda = 0.71073$  Å). The structures were solved by direct methods and refined on  $F^2$  by full-matrix least-squares methods using SHELXTL.<sup>15</sup>

CCDC reference number 186/1603.

See <http://www.rsc.org/suppdata/dt/1999/3393/> for crystallographic files in .cif format.

### Preparation of single crystals of the complex

$[\{\text{Mn}(\text{dmbpy})(\text{N}_3)_2\}_n] \mathbf{1}$ . To an aqueous solution (25 cm<sup>3</sup>) containing NaN<sub>3</sub> (2 mmol) and Mn(NO<sub>3</sub>)<sub>2</sub>·6H<sub>2</sub>O (1 mmol) was added a methanolic solution (10 cm<sup>3</sup>) of 4,4'-dimethyl-2,2'-bipyridine (dmbpy) (1 mmol). Yellow microcrystals precipitated in 10 min. The solid samples were filtered off and washed with methanol and diethyl ether (yield *ca.* 75%) (Found: C, 44.46; H, 3.70; Mn, 17.00; N, 34.56. Calc.: C, 44.55; H, 3.71; Mn, 17.01; N, 34.65%). IR:  $\tilde{\nu}_{\text{max}}/\text{cm}^{-1}$  2140, 2094 and 2056 ( $\nu_{\text{asym}} \text{N}_3$ ).

Yellow slab crystals suitable for X-ray single crystal analysis were obtained by slow evaporation of the above filtrate in the air.

$[\{\text{Cu}(\text{dmbpy})(\text{N}_3)_2\}_n] \mathbf{2}$ . This compound was prepared as green block crystals in a way similar to that of **1**. Yield *ca.* 80% (Found: C, 43.46; H, 3.70; Cu, 19.21; N, 33.58. Calc.: C, 43.39; H, 3.62; Cu, 19.14; N, 33.75%). IR:  $\tilde{\nu}_{\text{max}}/\text{cm}^{-1}$  2080 and 2047 ( $\nu_{\text{asym}} \text{N}_3$ ).

## Results and discussion

The complexes **1** and **2** were obtained as crystals when M<sup>2+</sup> (M = Mn or Cu) reacted with NaN<sub>3</sub> and 4,4'-dimethyl-2,2'-bipyridine in aqueous solution. The synthetic method has been commonly used to prepare azide-bridged complexes of different structures.

### Structure of complex 1

The ORTEP<sup>16</sup> drawing and a view of the unit cell of the two-dimensional  $[\{\text{Mn}(\text{dmbpy})(\text{N}_3)_2\}_n]$  complex are shown in Figs.

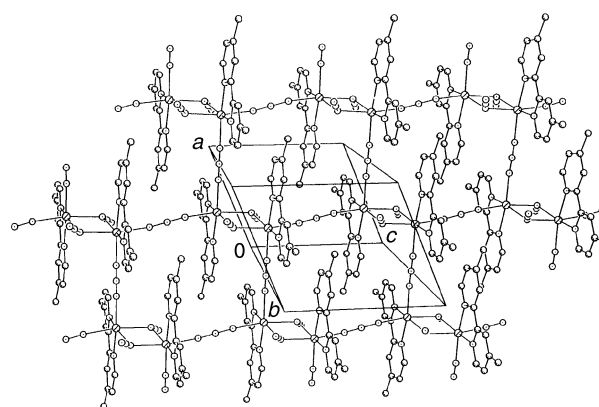


Fig. 2 View of the unit cell of  $[\{\text{Mn}(\text{dmbpy})(\text{N}_3)_2\}_n] \mathbf{1}$ .

**1** and **2**, respectively. Selected bond distances and angles with their estimated standard deviations are listed in Table 2.

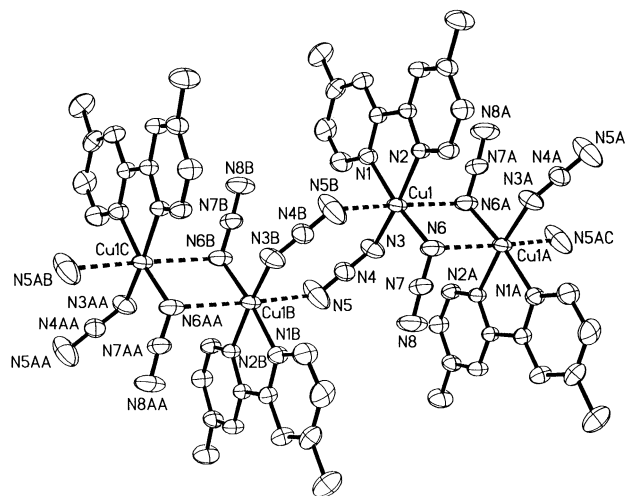
The structure of a dimanganese unit is shown in Fig. 1. Each manganese(II) ion has a distorted octahedral geometry, completed by the two nitrogen atoms of the dmbpy ligand [Mn–N1, N2; 2.238(2), 2.285(2) Å], two end-on [Mn–N3, N3A; 2.336(2), 2.203(2) Å] and two end-to-end [Mn–N6, N8; 2.223(2), 2.147(2) Å] azide nitrogen atoms. The two manganese(II) ions in the dimer are linked by two end-on azide groups which extend through the two end-to-end azide ligands to the other two dimer units forming a two-dimensional network (Fig. 2). Then, each manganese atom has three neighboring manganese atoms bridged by azide ligands. The Mn···Mn distance through the EO azide bridges is 3.5334(5) Å, and that through EE azide is 6.611(5) Å along the *c* direction and 6.537(5) Å in the other direction. The four atoms Mn(1), Mn(1A), N(3) and N(3A) are coplanar. The EO bridging azides, which are quasi-linear [N3–N4–N5 178.9(3)°], slightly deviate (up and down) from that plane. The Mn(1)–N(3)–Mn(1A) angle in the EO mode is 102.18(8)°, which lies in the typical range for this kind of bridge. For the EE bridges the Mn(1)–N(8)–N(9) angle is 163.8(2)° and Mn(1)–N(6)–N(7) is 153.9(2)°. The two EE bridges of the manganese(II) ion are quasi-perpendicular to each other with the angle of 93.58(9)° [N(8)–Mn–N(6)].

### Structure of complex 2

An ORTEP drawing and a view of the unit cell of the copper chain are shown in Figs. 3 and 4, respectively. Selected bond distances and angles are listed in Table 3.

**Table 1** Summary of crystallographic data for complexes **1** and **2**

	<b>1</b>	<b>2</b>
Empirical formula	C <sub>24</sub> H <sub>24</sub> Mn <sub>2</sub> N <sub>16</sub>	C <sub>12</sub> H <sub>12</sub> CuN <sub>8</sub>
<i>M</i>	646.47	331.84
Crystal system	Monoclinic	Triclinic
Space group	<i>P</i> 2 <sub>1</sub> / <i>n</i>	<i>P</i> 1̄
<i>a</i> /Å	7.8380(2)	7.9610(6)
<i>b</i> /Å	19.8698(5)	9.3836(1)
<i>c</i> /Å	9.5558(3)	10.7626(8)
<i>α</i> /°		113.439(1)
<i>β</i> /°	111.932(1)	101.228(1)
<i>γ</i> /°		101.982(1)
<i>U</i> /Å <sup>3</sup>	1380.51(7)	686.89(8)
<i>Z</i>	2	2
<i>D</i> <sub>c</sub> /g cm <sup>-3</sup>	1.555	1.604
<i>μ</i> /mm <sup>-1</sup>	0.963	1.596
No. reflections (total)	8896	4892
unique	3170	3352
observed [ <i>I</i> > 2σ( <i>I</i> )]	2497	2755
Parameters	241	192
Structure solution	SHELXTL (1997)	SHELXTL (1996)
Final <i>R</i> [ <i>I</i> > 2σ( <i>I</i> )]	0.0348	0.0452
(all data)	0.0543	0.0582

**Fig. 3** An ORTEP drawing (30% thermal probability ellipsoids) of [*n* Cu(dmbpy)(N<sub>3</sub>)<sub>2</sub>]<sub>n</sub> **2** showing the atom numbering.

The crystal structure of complex **2** consists of chains of copper(II) ions alternatively bridged by asymmetric double end-on and end-to-end azide groups (Fig. 4). The co-ordination geometry around each copper(II) ion is a distorted octahedron. The equatorial positions are occupied by four nitrogen atoms: two from the dmbpy ligand and two from azide groups (Fig. 3), whereas the apical sites are occupied by azide nitrogens from the neighboring units. Thus one of the two azide ligands in each unit acts as an EO bridge and the other as an EE bridge through which the neighboring units are connected leading to a neutral copper chain. The EO and EE bridges are alternately arranged. The Cu–N (dmbpy) bond lengths (average 2.027(2) Å) are in agreement with those reported for bipy-containing copper(II) complexes<sup>14,17–21</sup> and slightly longer than the other two equatorial Cu–N (azide) bonds [average 1.989(3) Å]. The values of the two apical Cu–N (azide) bonds are longer than the equatorial ones [2.632(3) and 2.532(5) Å for Cu(1)–N(6a) and Cu(1)–N(5b)] showing the existence of both asymmetric end-on and end-to-end azide bridges. The four equatorial atoms N(1), N(2), N(6) and N(3) are coplanar. The Cu(1)–N(6A)–Cu(1A) angle in the EO mode is 97.0°. For the EE bridges the Cu(1)–N(5B)–N(4B) angle is 136.5° and Cu(1)–N(3)–N(4) is 125.1°. The Cu···Cu distance through EO azide is 3.4903(3) Å and that through EE azide is 5.433 Å.

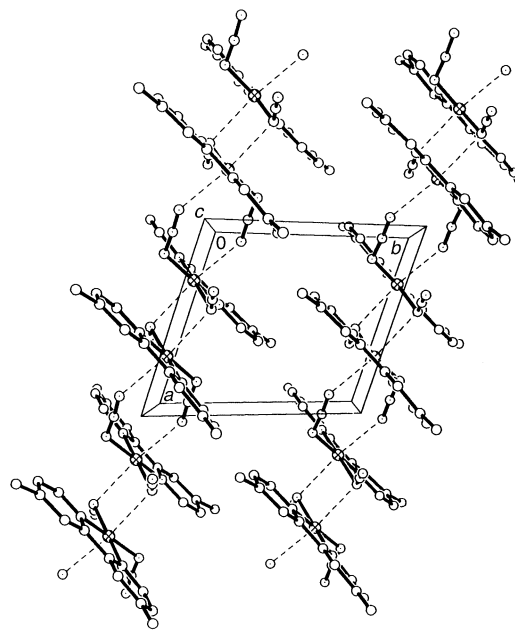
**Table 2** Selected bond lengths (Å) and angles (°) for complex **1**

Mn(1)–N(8)	2.147(2)	Mn(1)–N(3A)	2.203(2)
Mn(1)–N(6)	2.223(2)	Mn(1)–N(1)	2.238(2)
Mn(1)–N(2)	2.285(2)	Mn(1)–N(3)	2.336(2)
N(3)–Mn(1A)	2.203(2)	N(3)–N(4)	1.190(3)
N(5)–N(4)	1.143(3)	N(6)–N(7)	1.162(2)
N(7)–N(6B)	1.162(2)	N(8)–N(9)	1.152(2)
N(9)–N(8C)	1.152(2)	Mn(1)···Mn(1A)	3.5334(5)
N(1)–Mn(1)–N(2)	71.93(6)	N(8)–Mn(1)–N(6)	93.58(9)
N(1)–Mn(1)–N(6)	88.65(8)	N(2)–Mn(1)–N(3)	87.41(7)
N(8)–Mn(1)–N(3A)	101.76(8)	N(3)–Mn(1)–N(3A)	77.82(8)
N(3)–Mn(1)–N(8)	93.71(8)	Mn(1)–N(3)–Mn(1A)	102.18(8)
N(3A)–Mn(1)–N(1)	94.23(7)	N(6)–N(7)–N(6B)	180.0
N(8C)–N(9)–N(8)	180.0	N(5)–N(4)–N(3)	178.9(3)
N(4)–N(3)–Mn(1A)	125.7(2)	N(4)–N(3)–Mn(1)	118.3(2)
N(7)–N(6)–Mn(1)	153.9(2)	N(9)–N(8)–Mn(1)	163.8(2)

Symmetry codes: (A) 1 – *x*, –*y*, –*z* + 1; (B) –*x*, –*y*, –*z*; (C) –*x* + 1, –*y*, –*z* + 1.

**Table 3** Selected bond lengths (Å) and angles (°) for complex **2**

Cu(1)–N(3)	1.987(3)	Cu(1)–N(6)	1.990(3)
Cu(1)–N(2)	2.023(2)	Cu(1)–N(1)	2.031(2)
N(3)–N(4)	1.117(4)	N(4)–N(5)	1.171(5)
N(6)–N(7)	1.199(4)	N(7)–N(8)	1.139(4)
N(3)–Cu(1)–N(6)	95.62(12)	N(2)–Cu(1)–N(1)	79.22(9)
N(3)–Cu(1)–N(2)	171.23(11)	N(6)–Cu(1)–N(2)	92.82(10)
N(3)–Cu(1)–N(1)	92.25(11)	N(6)–Cu(1)–N(1)	171.81(10)
N(4)–N(3)–Cu(1)	125.1(3)	N(7)–N(6)–Cu(1)	121.3(2)
N(5)–N(4)–N(3)	175.3(4)	N(8)–N(7)–N(6)	176.5(4)

**Fig. 4** View of the unit cell of [*n* Cu(dmbpy)(N<sub>3</sub>)<sub>2</sub>]<sub>n</sub> **2**.

### IR and EPR spectra

The IR spectral data of the complexes given in the Experimental section show three sharp bands at 2140, 2094 and 2056 cm<sup>-1</sup> for **1** and two sharp bands at 2080 and 2047 cm<sup>-1</sup> for **2**. These data are consistent with the occurrence of both end-on and end-to-end bridging azides in the two complexes.<sup>8,14</sup>

The X-band powder EPR spectrum of complex **1** at room temperature shows an isotropic signal at *g* = 2.0 and that of **2** at room temperature is rhombic with *g*<sub>1</sub> = 2.220, *g*<sub>2</sub> = 2.077 and *g*<sub>3</sub> = 2.042. The spectra do not change significantly upon cooling to 110 K, which indicates that the co-ordination mode does not alter to a great extent.

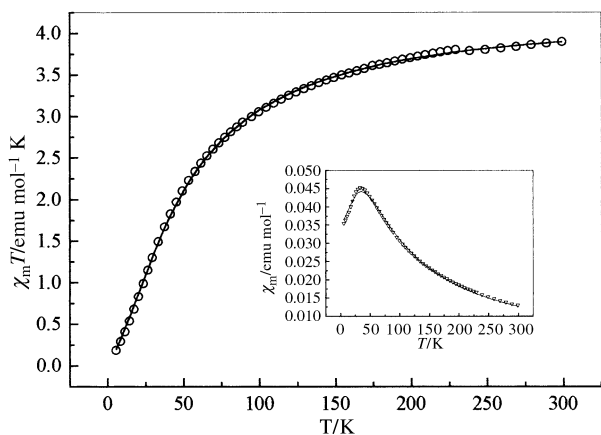


**Fig. 5** Thermal variation of  $\chi_m T$  (○) and  $\chi_m$  (▽) for compound **1**. The solid line corresponds to the best theoretical fit (see text).

### Magnetic properties

Variable temperature magnetic susceptibility measurements of complexes **1** and **2** have been performed on polycrystalline samples in the temperature range 5–300 K. The magnetic behavior is represented in the  $\chi_m T$  vs.  $T$  fashion in Figs. 5 and 6, respectively. The inserts show the thermal dependence of the magnetic susceptibility;  $\chi_m$  is the corrected molar magnetic susceptibility per Mn (**1**) or per Cu (**2**).

**Complex 1.** The  $\chi_m$  value increases as the temperature decreases, reaching a rounded maximum at 32 K, and then decreases to 5 K. At room temperature the  $\chi_m T$  value is 3.91 emu mol<sup>-1</sup> K (5.59  $\mu_B$ ), which is smaller than that expected for an uncoupled manganese(II) ion (5.91  $\mu_B$ ). This value decreases with decreasing temperature.

According to the structural data, this compound should exhibit alternating ferro- and antiferro-magnetic interactions through the double EO and single EE bridges, respectively. Ferromagnetic interactions promoted by the double EO bridges have been observed in the binuclear complex [ $\{\text{Mn}(\text{N}_3)_2(\text{terpy})\}_2 \cdot 2\text{H}_2\text{O}$  (terpy = 2,2':6',2''-terpyridine),<sup>22</sup> also in the 1-D compound [ $\text{Mn}(\text{bpy})(\text{N}_3)_2$ ] (bpy = 2,2'-bipyridine)<sup>1,8,9</sup> and 2-D compound [ $\text{Mn}_2(\text{bpym})(\text{N}_3)_4$ ] (bpym = 2,2'-bipyrimidine);<sup>3</sup> all of them have EO azide bridges ( $J = 3.5$ , 13.8 and  $zJ' = 2.87$  K, respectively). While antiferromagnetic interactions promoted by the double EE bridges have been found in the 1-D compound [ $\text{Mn}(\text{bpy})(\text{N}_3)_2$ ],<sup>23</sup> the 1-D compound [ $\{\text{Mn}(3\text{-Etpy})_2(\text{N}_3)_2\}_n$ ] (3-Etpy = 3-ethylpyridine) and [ $\{\text{Mn}(2\text{-pyOH})_2(\text{N}_3)_2\}_n$ ] (2-pyOH = 2-hydroxypyridine)<sup>24</sup> and 2-D compound [ $\{\text{Mn}(4\text{acpy})_2(\text{N}_3)_2\}_n$ ] (4acpy = 4-acetylpyridine)<sup>4</sup> all have EE azide bridges ( $J = -17.01$ ,  $-19.88$ / $-16.86$ ,  $-14.52$  and  $-5.52$  K, respectively). Compound **1** should thus be classified as an alternating 2-D ferro-antiferromagnetic system.

Antiferromagnetic interaction becomes evident from the maximum in the  $\chi_m$  vs.  $T$  plot, and a greater  $J_{\text{AF}}$  should also be assumed for compound **1**. Evaluation of the superexchange coupling constants in the paramagnetic region is not possible for a manganese 2-D system where several coupling pathways are operative.<sup>4</sup> In order to correlate molecular structures with magnetic properties, we employed two simple models as an approximate approach. The first was based on a Hamiltonian type uniform chain formed by the zigzag end-to-end bridges, eqn. (1), where  $J$  was treated as the intrachain exchange con-

$$\chi_{\text{chain}} = C(1 + \mu)/(1 - \mu) \quad (1)$$

$$C = Ng^2\mu_B^2 S(S+1)/3kT; \mu = \coth(K) - (1/K)$$

$$K = JS(S+1)/kT; S = 5/2$$

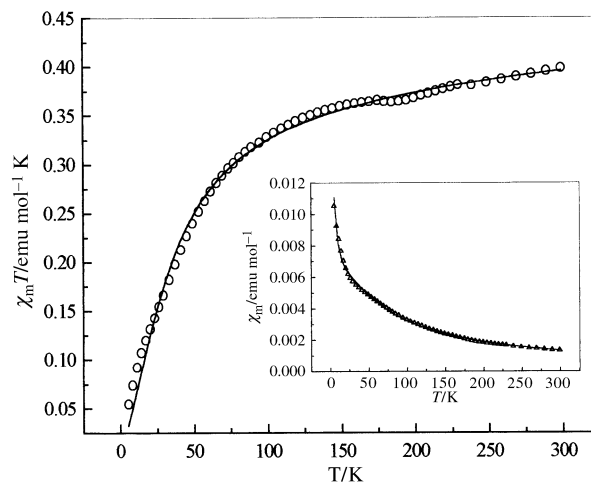


**Fig. 6** Thermal variation of  $\chi_m T$  (○) and  $\chi_m$  (△) for compound **2**. Details as in Fig. 5.

stant. Then the interactions promoted by the double end-on bridges were treated as interchain interactions with the molecular field approximation,<sup>24,25</sup> eqn. (2), where  $J'$  is the interchain

$$\chi = \chi_{\text{chain}}/[1 - \chi_{\text{chain}}(2zJ'/Ng^2\mu_B^2)] \quad (2)$$

coupling constant and  $z$  the number of interacting neighbors, 2 in this case. In the second model, ferromagnetic dimers antiferromagnetically coupled to each other were considered,<sup>26</sup> eqn. (3). In this case  $J$  was the exchange constant promoted by the

$$\chi = \chi_{\text{dimer}}/[1 - \chi_{\text{dimer}}(2zJ'/Ng^2\mu_B^2)] \quad (3)$$

double EO bridges,  $J'$  is the coupling constant promoted by the single EE azide group and  $z$  is 4.

The best fit for both  $\chi_m$  and  $\chi_m T$  with the first model (shown in Fig. 5) leads to the following parameters:  $J/k = -7.7$  K,  $zJ'/k = 2.5$  K,  $g = 2.0$  and  $R = 3.0 \times 10^{-4}$  ( $R = \Sigma[(\chi_m)_{\text{obs}} - (\chi_m)_{\text{calc}}]^2/\Sigma[(\chi_m)_{\text{obs}}]^2$ ) and with the second model to  $J/k = 24.54$  K,  $zJ'/k = -12.06$  K,  $g = 1.93$  and  $R = 4.9 \times 10^{-4}$ . From these results, and considering their limitations, the first model proposed shows that the antiferromagnetic interactions are predominant in compound **1** as predicted from the  $\chi_m$  vs.  $T$  plot in Fig. 5. It also appears to provide a very good description of the susceptibility in the range 5–300 K and is in good agreement with the results from the EPR measurements.

**Complex 2.** The  $\chi_m$  value increases as the temperature decreases from 0.00136 emu mol<sup>-1</sup> at room temperature to 0.01 emu mol<sup>-1</sup> at 4.75 K. At room temperature, the  $\chi_m T$  value is 0.4 emu mol<sup>-1</sup> K (1.79  $\mu_B$ ), which is characteristic of a magnetically isolated spin doublet. This value decreases smoothly as the temperature decreases, attaining a value of 0.056 emu mol<sup>-1</sup> K at 4.75 K.

The structure of compound **2** shows the regular alternating asymmetric double end-on and double end-to-end azide bridges, the Cu...Cu separations being 3.4903(3) and 5.433(3) Å, respectively. According to the structure data and considering its magnetic properties, the structure of **2** is similar to that of [ $\text{Mn}(\text{bipy})(\text{N}_3)_2$ ]. We tried to evaluate the magnetic data through the alternating ferro- and antiferro-magnetic chain model with the spin Hamiltonian:<sup>27</sup>  $H = -J_1 \Sigma \mathbf{S}_{2i} \cdot \mathbf{S}_{2i+1} - J_2 \Sigma \mathbf{S}_{2i+1} \cdot \mathbf{S}_{2i+2}$  where  $J_1$  is the coupling constant for the EO bridge and  $J_2$  that for the EE bridge.

The best fit for both  $\chi_m$  and  $\chi_m T$  (shown in Fig. 6) has the parameters:  $J_1/k = 11$  K,  $J_2/k = -87$  K,  $g = 2.06$  and  $R = 6 \times 10^{-5}$ . The model provides an excellent fit as indicated by the low value of  $R$ .

## Acknowledgements

This work was supported by state key project of Fundamental Research and the National Nature Science Foundation of China, by the University of Hong Kong and the Malaysian Government research grant R&D No. 190-9609-2801.

## References

- 1 R. Cortes, L. Lezama, J. L. Pizarro, M. I. Arriortua, X. Solans and T. Rojo, *Angew. Chem., Int. Ed. Engl.*, 1994, **33**, 2488.
- 2 G. De Munno, M. Julve, G. Viau, F. Lloret, J. Faus and D. Viterbo, *Angew. Chem., Int. Ed. Engl.*, 1996, **35**, 1807.
- 3 R. Cortes, L. Lezama, J. L. Pizarro, M. I. Arriortua, X. Solans and T. Rojo, *Angew. Chem., Int. Ed. Engl.*, 1996, **35**, 1810.
- 4 A. Escuer, R. Vicente, M. A. S. Goher and F. A. Mautner, *Inorg. Chem.*, 1997, **36**, 3440.
- 5 R. Vicente, A. Escuer, J. Ribas and X. Solans, *Inorg. Chem.*, 1992, **31**, 1726.
- 6 J. Ribas, M. Monfort, X. Solans and M. Drillon, *Inorg. Chem.*, 1994, **33**, 742.
- 7 G. D. Munno, M. Julve, F. Lloret, J. Faus, M. Verdaguer and A. Caneschi, *Angew. Chem., Int. Ed. Engl.*, 1993, **32**, 1046.
- 8 R. Cortes, M. Drillon, X. Solans, L. Lezama and T. Rojo, *Inorg. Chem.*, 1997, **36**, 677.
- 9 G. Viau, M. G. Lombardi, G. D. Munno, M. Julve, F. Lloret, J. Faus, A. Caneschi and J. M. C. Juan, *Chem. Commun.*, 1997, 1195.
- 10 G. D. Munno, T. Poerio, G. Viau, M. Julve, F. Lloret, Y. Journaux and E. Riviere, *Chem. Commun.*, 1996, 2587.
- 11 G. D. Munno, M. Julve, F. Lloret, J. Faus, M. Verdaguer and A. Caneschi, *Angew. Chem., Int. Ed. Engl.*, 1993, **32**, 1046.
- 12 R. Cortes, L. Lezama, J. L. Pizarro, M. I. Arriortua, X. Solans and T. Rojo, *Angew. Chem., Int. Ed. Engl.*, 1994, **106**, 2520.
- 13 M. F. Charlot, O. Kahn, M. Chaillet and C. Larrieu, *J. Am. Chem. Soc.*, 1986, **108**, 2574.
- 14 G. D. Munno, M. G. Lombardi, M. Julve, F. Lloret and J. Faus, *Inorg. Chim. Acta*, 1998, **282**, 82.
- 15 G. M. Sheldrick, SHELXTL, University of Göttingen, 1996.
- 16 C. K. Johnson, ORTEP II, Report ORNL-5138, Oak Ridge, National Laboratory, Oak Ridge, TN, 1976.
- 17 J. Cano, G. De Menno, J. L. Sanz, R. Ruiz, J. Faus, F. Lloret, M. Julve and A. Caneschi, *J. Chem. Soc., Dalton Trans.*, 1997, 1915.
- 18 R. Ruiz, F. Lloret, M. Julv, M. C. Munoz and C. Bois, *Inorg. Chim. Acta*, 1994, **219**, 179.
- 19 I. Castro, J. Sletten, J. Faus and M. Julve, *J. Chem. Soc., Dalton Trans.*, 1992, 2271.
- 20 H. Okawa, M. Koikawa, S. Kida, D. Lineau and H. Oshio, *J. Chem. Soc., Dalton Trans.*, 1990, 469.
- 21 X. Solans, M. Aguiló, A. Gleizes, J. Faus, M. Julve and M. Verdaguer, *Inorg. Chem.*, 1990, **29**, 775.
- 22 R. Cortes, L. Pizarro, L. Lezama, M. S. Arriortua and T. Rojo, *Inorg. Chem.*, 1994, **33**, 2697.
- 23 A. Escuer, R. Vicente, M. A. S. Goher and F. A. Mautner, *Inorg. Chem.*, 1995, **34**, 5707.
- 24 A. Escuer, R. Vicente, M. A. S. Goher and F. A. Mautner, *Inorg. Chem.*, 1998, **37**, 782.
- 25 M. E. Fisher, *Am. J. Phys.*, 1964, **32**, 343.
- 26 J. H. Van Vleck, *Electrical and Magnetic Susceptibilities*, Oxford University Press, 1965.
- 27 J. J. Borrás-Almenar, E. Coronado, J. Curely, R. Georges and J. C. Gianduzzo, *Inorg. Chem.*, 1994, **33**, 5171.

Paper 9/03968F